

“NOTICE: this is the author’s version of a work that was accepted for publication in Polymer Testing. Changes resulting from the publishing process, such as peer review, editing, corrections, structural formatting, and other quality control mechanisms may not be reflected in this document. Changes may have been made to this work since it was submitted for publication. A definitive version was subsequently published in POLYMER TESTING, VOL 31, ISSUE 4, JUNE 2012, PAGES 512-519, DOI: [10.1016/j.polymertesting.2012.02.010](https://doi.org/10.1016/j.polymertesting.2012.02.010)”

## **Ballistic performance of thermoplastic composite laminates made from aramid woven fabric and polypropylene matrix**

J.G. Carrillo<sup>a,\*</sup>, R.A. Gamboa<sup>a</sup>, E.A. Flores-Johnson<sup>b</sup>, P.I. Gonzalez-Chi<sup>a</sup>

<sup>a</sup>Centro de Investigacion Cientifica de Yucatan, A.C., Unidad de Materiales, C. 43, No. 130, Chuburna de Hgo., C.P. 97200, Merida, Mexico.

<sup>b</sup>Institute of Materials Engineering, Australian Nuclear Science and Technology Organisation, Locked Bag 2001, Kirrawee DC, NSW 2232, Australia.

\*Corresponding author: Tel. +52 9999428330, Fax. +52 9999813900, E-mail: [jgcb@cicy.mx](mailto:jgcb@cicy.mx)

### **Abstract**

In this paper, the ballistic behavior of multi-layer Kevlar<sup>®</sup> aramid fabric/polypropylene (PP) composite laminate (CL) and plain layered aramid fabric (AF) impact specimens was investigated. It was found that the thermoplastic PP matrix increases the ballistic performance of CL targets when compared to AF targets with similar areal density, resulting in less aramid fabric needed to obtain the same level of protection when the PP matrix is incorporated. It was found that the improved ballistic performance of CL targets is due to the fact that the thermoplastic matrix enables energy-absorbing mechanisms such as fabric/matrix debonding and delamination. The ballistic limit and penetration threshold energy of the CL configurations, which were predicted using an empirical model, were found to be higher than those of the AF targets. These results show that aramid fabric/PP laminates should be further studied for improved ballistic performance at lower costs.

**Keywords:** Aramid fabric; thermoplastic matrix; composite laminate; ballistic resistance; lightweight armor.

## 1. Introduction

Currently, high-strength polymer fabrics are widely used for protective systems due to their mechanical properties and impact resistance [1]. High-performance polymer fibers such as aramid fiber (aromatic polyamide), ultra-high molecular weight polyethylene (UHMWPE) fibers and Zylon<sup>®</sup> poly (p-phenylene-2,6-benzobisoxazole) fibers have remarkable properties such as lightness, flexibility, high Young's modulus and good impact resistance, which make them attractive candidates for the manufacturing of modern protective equipment.

Fiber-reinforced polymer composites (FRPC's) have been widely used for protective structures, particularly those with high-performance fibers [2]. When FRPC's are intended to be used for lightweight ballistic protection or soft armor, weak fiber-matrix adhesion is required to allow the fibers maximum deformation [3], thus absorbing more impact energy. In this case, thermoplastic polymers have an advantage over thermosetting matrices, which are known for their high stiffness and low deformation [2, 4]. It has been shown that by adding limited amounts of thermoplastic resin to the fabric, an improvement in the impact resistance can be obtained [5] because the thermoplastic matrix maintains the orientation and position of the fibers during an impact event and distributes the load caused by the impact among the fibers [2]. In laminate composites the matrix enables delamination and debonding, which are energy-absorbing mechanisms [6, 7]. The matrix may also protect the fibers from environmental factors such as the reduction of impact resistance under conditions of high humidity [8] and the reduction of mechanical properties due to photo-degradation caused by ultra-violet radiation [9, 10].

One of the most well-known polymeric fibers for protective systems is aramid fiber with the commercial name Kevlar<sup>®</sup> [5]. Fabrics made with this aramid fiber have high strength, high modulus and good tenacity, which are desirable properties for ballistic applications; however, they are relatively expensive [5] and the design of protective equipment with these fabrics should include studies to reduce the amount of required fabric layers without compromising the effectiveness of the armor. Although there are studies of the ballistic performance of aramid/thermosetting matrix systems [11, 12], the available experimental data in open literature for aramid/thermoplastic matrix composites is limited. Moreover, aramid/polypropylene systems have not been studied in detail despite the fact that polypropylene (PP) is inexpensive and exhibits low adhesion to aramid fiber [6, 13], which is desirable for soft armor. Mayo Jr. et al. [14] reported that PP-impregnated aramid fabric exhibits an improvement in dynamic stab-resistance when compared to plain aramid fabric. However, studies on aramid/PP systems are not conclusive and more research on these thermoplastic systems should be carried out to fully understand their potential as lightweight armor.

This study is motivated by the lack of knowledge in the study of aramid fiber fabric composite laminates with thermoplastic PP matrix for ballistic protection. In this work, multi-layer aramid fabric/PP matrix composite laminates were fabricated and their impact resistance was studied and compared to multi-layer aramid fabric systems without a PP matrix. The contribution of the PP matrix to the system ballistic resistance is discussed. The mechanical properties of the laminate constituent materials are also reported. The mechanisms of impact energy absorption of composite laminates and plain aramid fabrics are discussed and analyzed by optical microscopy. The ballistic limit and perforation threshold

energy of the target configurations are predicted using an empirical model. Materials and experimental procedures are described in Section 2. Results and discussion are presented in Section 3, followed by conclusions in Section 4.

## 2. Experimental

### 2.1. Materials and impact specimen configurations

Two configurations of impact specimens were tested: (i) multi-layer aramid fabric composite laminate (CL) targets made with a PP matrix; and (ii) multi-layer aramid fabric (AF) targets without a matrix. For both configurations, plain-woven Hexcel aramid style 720 fabric (Kevlar<sup>®</sup> 129 fiber, 1420 denier) was used. Atactic PP films from Indelpro Company with a thickness of 0.032 mm and density of 910 kg/m<sup>3</sup> were used for the laminate specimens. The tensile mechanical properties of Kevlar<sup>®</sup> 129 yarns extracted from the fabric and PP films were measured in accordance to ASTM D7269 and ASTM D638 standards, respectively. Three specimens were tested for each material.

### 2.2 Fabrication of CL and AF impact specimens

The CL impact specimens were fabricated using layers of aramid fabric and PP films of 100×100 mm<sup>2</sup> as shown in Fig. 1a. Three films of PP were used between aramid fabric layers and for the outermost faces (Fig. 1a). The specimens ranged from one to eight layers of fabric. The laminates were molded using a Carver hot press (Model Auto Series) with the fabrication parameters described in Section 3.2.

Multi-layer fabric specimens without a PP matrix were fabricated. For these specimens, only the edges of the fabric layers were consolidated with PP to allow clamping (Fig. 1b), leaving an 80×80 mm<sup>2</sup> area of fabric for impact. The specimens ranged from one to eight layers of fabric.

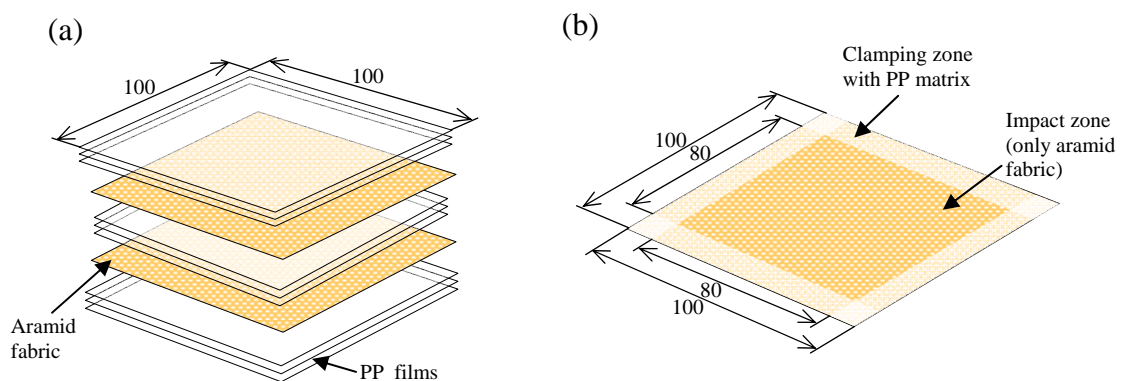


Fig. 1. Geometrical details of target configurations (dimensions are in mm) for: (a) composite laminates; and (b) plain multi-layer aramid fabric.

### 2.3. Impact tests setup

All samples were tested according to the NATO STANAG 2920 standard. The apparatus used for ballistic testing, which was designed and built in-house, comprises a pressure chamber, a barrel and a gas tank (Fig. 2). The firing system operates with pressurized nitrogen gas. The velocity of the projectile was measured with a Shooting Chrony

chronograph located between the barrel and the specimen. A steel frame with a window of  $80 \times 80 \text{ mm}^2$  was built to hold the sample without back support, as shown in Fig. 2. The specimens were fully clamped to the frame using bolts. A spherical steel projectile with a diameter of 6.7 mm and a mass  $m$  of 1.11 g was used. Six samples were tested per configuration; this methodology helped to obtain the ballistic limit, defined as the average velocity that at least 50% of samples reach the perforation threshold. Tests were performed under controlled conditions of temperature ( $24 \text{ }^\circ\text{C}$ ) and humidity (60%), keeping samples stable for 48 hours prior to the test to ensure repeatability of results.

The methodology used in this study to assess the ballistic performance of the impact specimens consists of establishing the ballistic limit of a five-layer AF target to use as reference impact velocity  $V_{ref}$ , and fixing the initial impact velocity to that value in all tests to determine the number of fabric layers that are necessary to fully stop the projectile for both CL and AF specimens. The reference impact velocity obtained was  $V_{ref} = 274.5 \text{ m/s}$ .

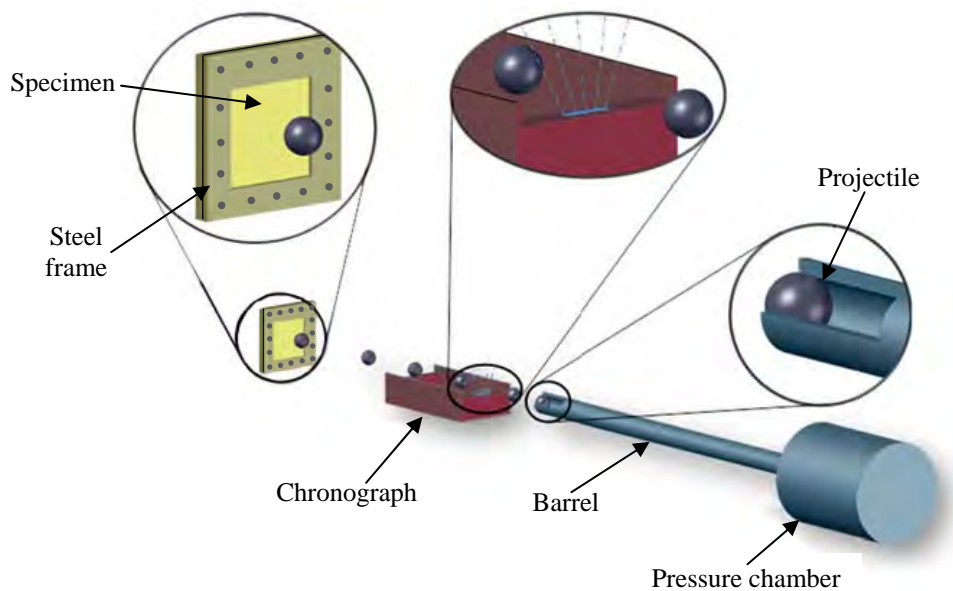


Fig. 2. Ballistic testing setup.

### 2.5. Microscopy of tested specimens

Post-test examination of selected specimens was performed with an optical microscope, model Leica DM LM, to identify energy-absorbing failure mechanisms during impact. Cross-sections of selected samples at the impact region were embedded in epoxy resin. Once the resin cured, the encapsulated sample was cut and the surface was polished until a smooth finish was obtained, thus allowing a clear observation of the surface through the microscope.

## 3. Results and discussion

### 3.1. Mechanical properties of the aramid yarns and PP films

Figures 3a and b show the stress-strain curves of Kevlar 129<sup>®</sup> yarns and PP film, respectively. The tensile mechanical properties obtained from Fig. 3 are depicted in Table 1.

It can be seen that the mechanical properties of the Kevlar 129<sup>®</sup> yarns are lower than the mechanical properties reported by the manufacturer [15]. It is believed that although the yarns were extracted from the fabric with care, some of the fibers were damaged during the extraction process [16] or during the weaving process [17].

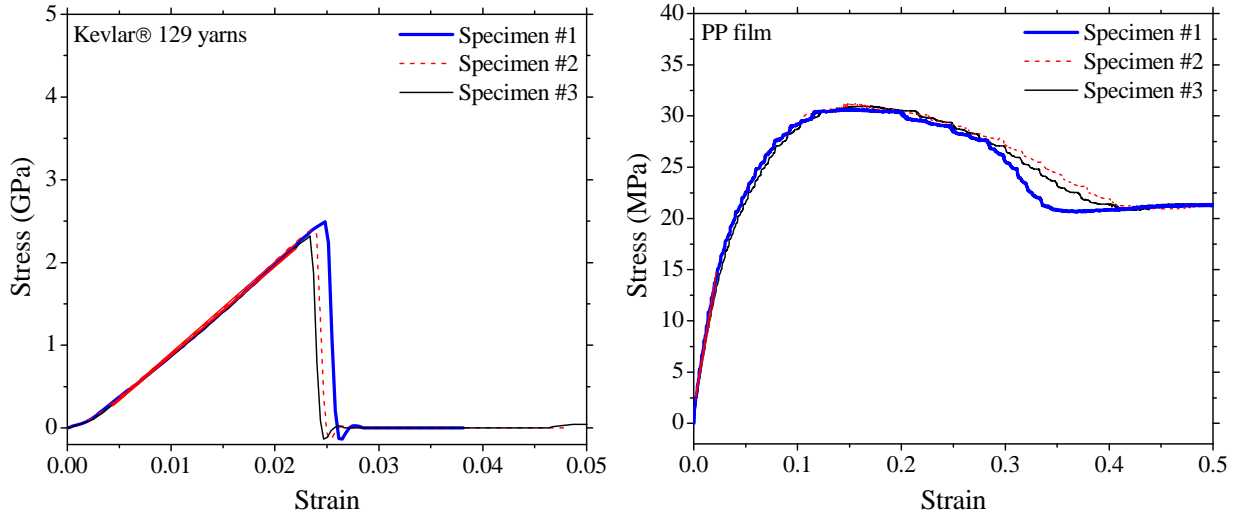


Fig. 3. Tensile mechanical properties of Kevlar<sup>®</sup> 129 fiber yarns and PP films.

Table 1. Tensile mechanical properties of the laminate constituents.

Material	Young's Modulus (GPa)	Tensile strength (GPa)	Failure strain
Kevlar <sup>®</sup> 129 yarn	108.54±1.09	2.39±0.096	0.024±0.0006
Polypropylene film	0.59±0.025	0.0309±0.00028	0.154±0.0065

### 3.2. Methodology for the fabrication of the CL

It was found that the processing parameters time and temperature have an effect on the ballistic resistance and are critical in the consolidation of the laminates. At a molding temperature of 175 °C or less, poor adhesion was observed between layers leading to excessive fabric/matrix debonding and delamination during impact testing (Fig. 4a). Poor interfacial adhesion was also observed, with molding times of less than 20 min. It was found that when the laminates were molded at a temperature of 185 °C for a period of 20 min with a pressure of 6.05 MPa, and a cooling time of 25 min using the cooling water system of the press, good fabric wet-out was observed and good-quality laminates were obtained. The improvement in the adhesion when using the chosen fabrication parameters was clearly observed after the impact tests depicted in Fig. 4b.

### 3.3. Impact tests

Figure 5 shows the permanent deflection of the different target configurations at the mid-point after impact versus the number of aramid layers of the target. For three-layer CL

targets, it was observed that the projectile fully stopped for all tests while it only stopped in two of the tests for the two-layer CL target, indicating that the ballistic limit of a two-layer CL target should be close to the reference impact velocity. This indicates a reduction of 40-60% of aramid fabric is needed to stop the projectile when a PP matrix is incorporated into the system. Figure 5 also shows that for both configurations, the permanent deformation increases almost linearly with the number of layers before the projectile is stopped by the target (perforation threshold). This phenomenon is explained by the fact that the ballistic limit of the target increases with an increase in the number of layers, due to an increase in the energy-absorbing capacity of the system (Sections 3.4 and 3.5). When the number of fabric layers is sufficient to dissipate 100% of the impact energy of the projectile (two or three layers for CL targets and five layers for AF targets), a further increase in the number of layers results in an almost linear reduction of the permanent deflection (Fig. 5).

A reduction in the permanent deformation is also observed for CL targets when compared to AF targets for a given number of layers (Fig. 5), which shows that the PP matrix increases the ballistic performance of the targets for a given number of fabric layers. This phenomenon is explained by the fact that the PP matrix enables more energy-absorbing failure mechanisms such as delamination and tension in secondary yarns [7] as discussed in the next section.

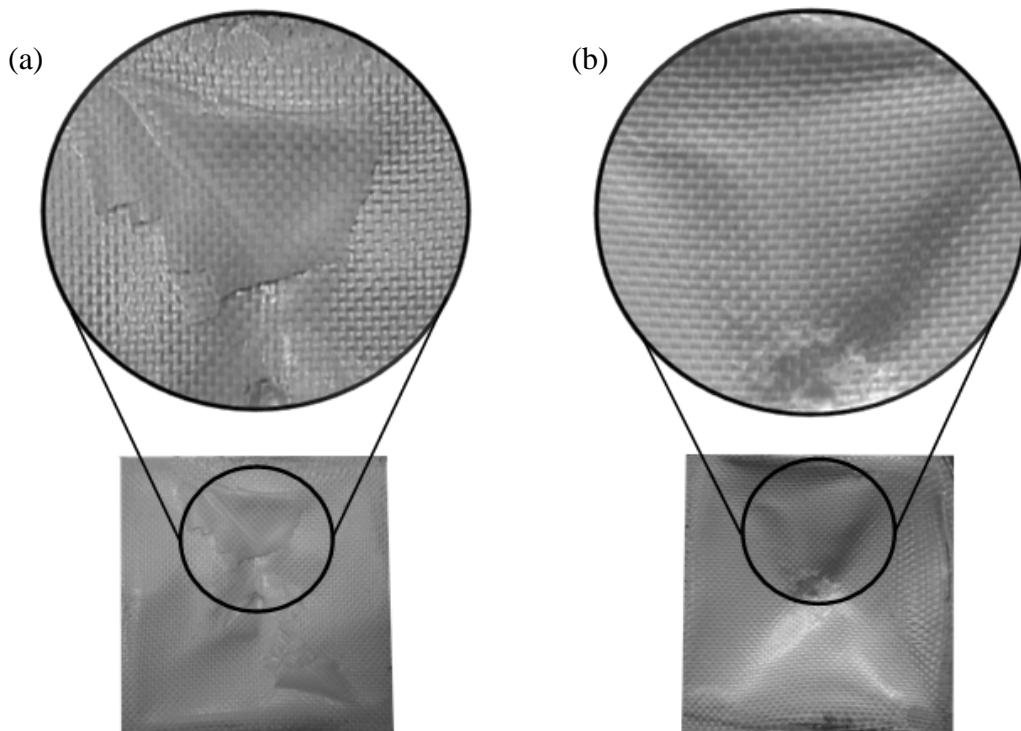


Fig. 4. (a) Fabric/matrix debonding on an impacted four-layer CL target; (b) Impacted four-layer CL target fabricated using optimal manufacturing parameters.

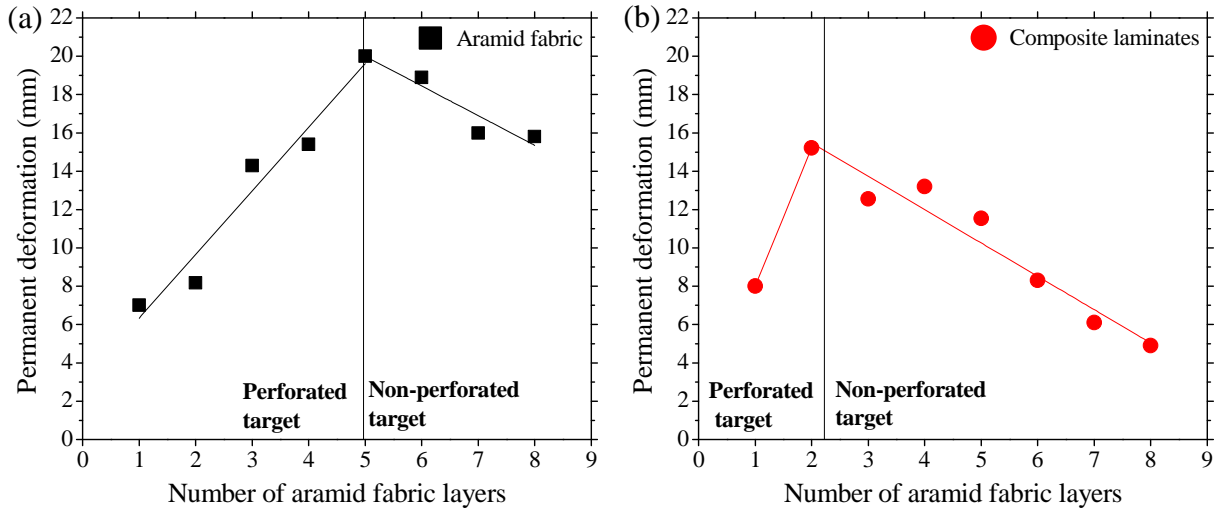


Fig. 5. Permanent deformation versus number of aramid fabric layers for: (a) Plain aramid fabric; and (b) composite laminates.

### 3.4. Failure modes

Figure 6 shows impacted three-layer CL and AF targets. The AF target has been completely perforated while the CL target has stopped the projectile (Fig. 5). It can be seen in Fig. 6 that although both targets have the same number of fabric layers, the failure modes observed in each configuration are very different due to the matrix incorporation in CL targets. For the AF target, the main energy-absorbing mechanism is straining of primary yarns, which are in direct contact with the projectile (Fig. 6a). These yarns stretch until they reach the maximum strain limit [18]. A pyramidal shape deformation is also observed (Fig. 6a) in the AF target due to the strain of the primary yarns, which form the inclined edges of the pyramid [19].

For CL targets, the matrix enables other mechanisms of energy absorption that are not observed in AF targets. Figure 6b shows fabric/matrix debonding and matrix cracking, which contribute to the absorption of impact energy. The deformation of secondary yarns in CL targets is greater than that of AF targets, which is due to the fact that the matrix produces a more even distribution of the target deformation [18]. Delamination was also observed, which is another energy-absorbing mechanism.

### 3.5. Microscopy of tested specimen

Figures 7a and b show a two-layer non-impacted and impacted composite laminate, respectively. A close-up view of the undamaged specimen (Figs. 7c and d) shows good PP impregnation into the fiber yarns, resulting in good matrix/fabric bonding. After impact testing, straining of primary yarns (Fig. 7e), delamination (Fig. 7f), matrix cracking (Fig. 7g) and fabric/matrix debonding (Fig. 7g) are identified as energy-absorbing mechanisms in CL targets.

**(a) Plain aramid fabric target (3 layers)**



**(b) Composite laminate target (3 layers)**

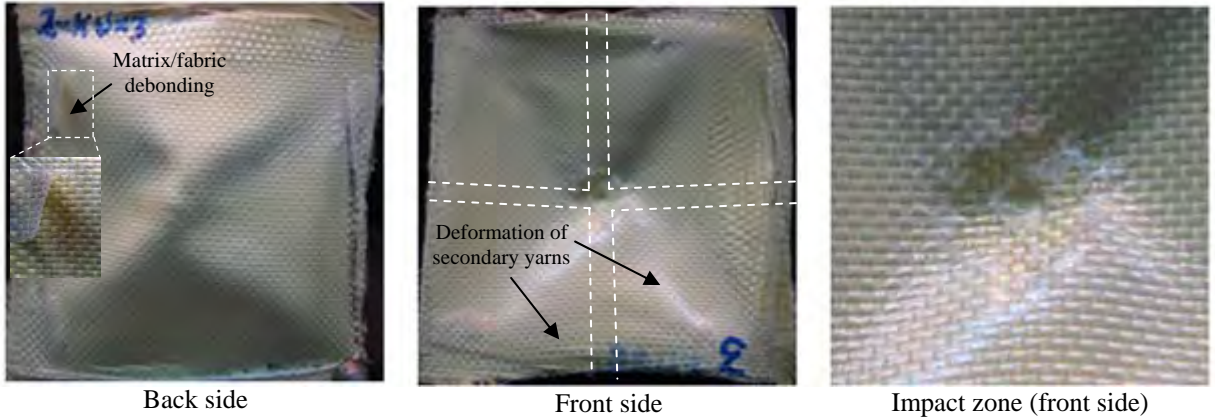


Fig. 6. Impact energy-absorbing mechanics for a four-layer (a) AF target and (b) CL target, impacted at 274.5 m/s.

**3.6 Prediction of the ballistic limit and perforation threshold energy**

It has been demonstrated by several researchers that the ballistic limit  $V_{bl}$  of a layered fabric system can be predicted by a simple empirical model of the form [20-22]:

$$V_{bl} = C\rho_A^n, \quad (1)$$

where  $C$  and  $n$  are material constants for a given type of fabric and  $\rho_A$  is the areal density. For AF targets, tensile fracture of primary yarns is the governing failure mechanism and thus  $n=0.5$  may be used [23]. This value has been used to predict  $V_{bl}$  of layered nylon/aramid systems [20]. The areal density of the fabric used in this study is  $\rho_A=0.261 \text{ kg/m}^2$  for a 0.37-mm thick single layer [15]. For this fabric, a value of  $C=240.3$  is found by using the ballistic limit of  $V_{bl}=274.5 \text{ m/s}$  for a five-layer AF target with  $\rho_A=1.305 \text{ kg/m}^2$  (Table 2) in Eq. 1. The predicted ballistic limit using Eq.1 for AF targets is plotted in Fig. 8a along with the experimental value of  $V_{bl}$  for a five-layer AF target.



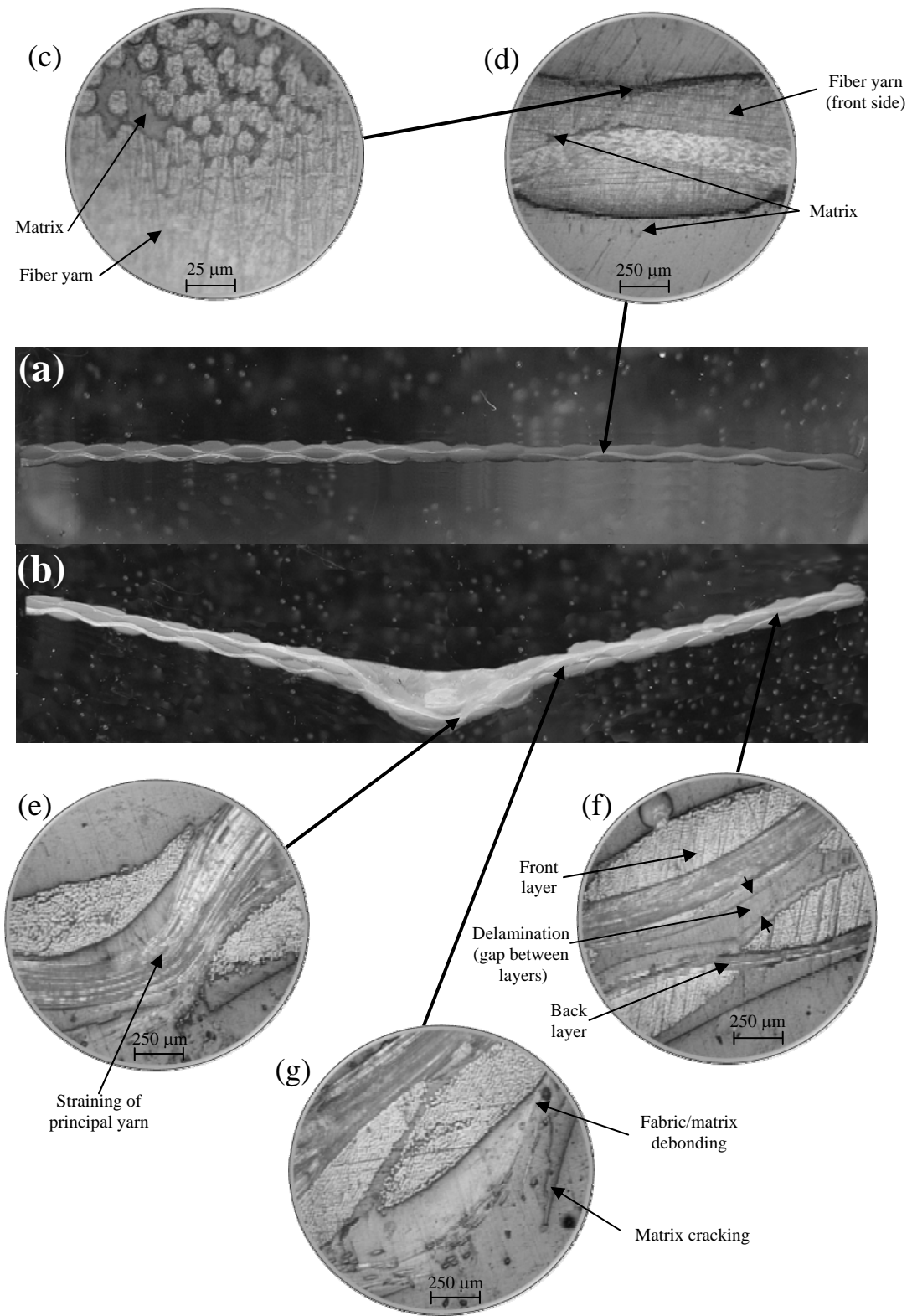


Fig. 7. Micrographs of a two-layer CL target: (a) Non-impacted specimen; (b) Impacted specimen; (c-d) close-up view of non-impacted specimen; (e-g) close-up view of impacted specimen.

Table 2. Areal density of impact specimen configurations.

Number of fabric layers	Areal density (kg/m <sup>2</sup> )	
	AF targets (calculated)	CL targets (measured)
1	0.261	0.325
2	0.522	0.718
2.5	-	0.783 <sup>1</sup>
3	0.783	0.907
4	1.044	1.224
5	1.305	1.426
6	1.566	1.810
7	1.827	1.964
8	2.088	2.404

<sup>1</sup>Theoretical value.

Equation 1 can also be used for composite targets [22, 23]; however, the constant  $n$  will depend on several factors such as the composite stiffness and failure mechanisms [23]. Values of  $n=0.42$  and  $0.56$  have been reported for aramid/phenolic-polyvinylbutyral [23] and aramid/phenolic [22, 24] composites, respectively. For CL targets,  $C$  is obtained by using  $V_{bl}=274.5$  m/s for a CL target with  $\rho_A=0.783$  kg/m<sup>2</sup> (2.5 layers, see Table 2) because it was observed in Section 3.3 that the  $V_{bl}$  of a two-layer CL target must be lower than  $V_{ref}$  but higher than  $V_{ref}$  for a three-layer CL target. This assumption is made considering that an almost linear dependency of the areal density on the number of layers is observed (Table 2). Different values of  $n$  were used ( $n=0.4, 0.5, 0.6$ ) to predict  $V_{bl}$  for CL targets (Fig. 8a). It can be seen that the predicted ballistic limit for a given areal density increases with an increase in  $n$ .

The perforation threshold energy  $E_{thr}$  of the configurations was predicted using the following [23]:

$$E_{thr} = 1/2mV_{bl}^2. \quad (2)$$

Figure 8b shows the predicted  $E_{thr}$  for all configurations. It can be seen that there is a linear dependency of  $E_{thr}$  on  $V_{bl}$  when  $n=0.5$ . An increase in the predicted  $E_{thr}$  for a given areal density is also observed when  $n$  increases.

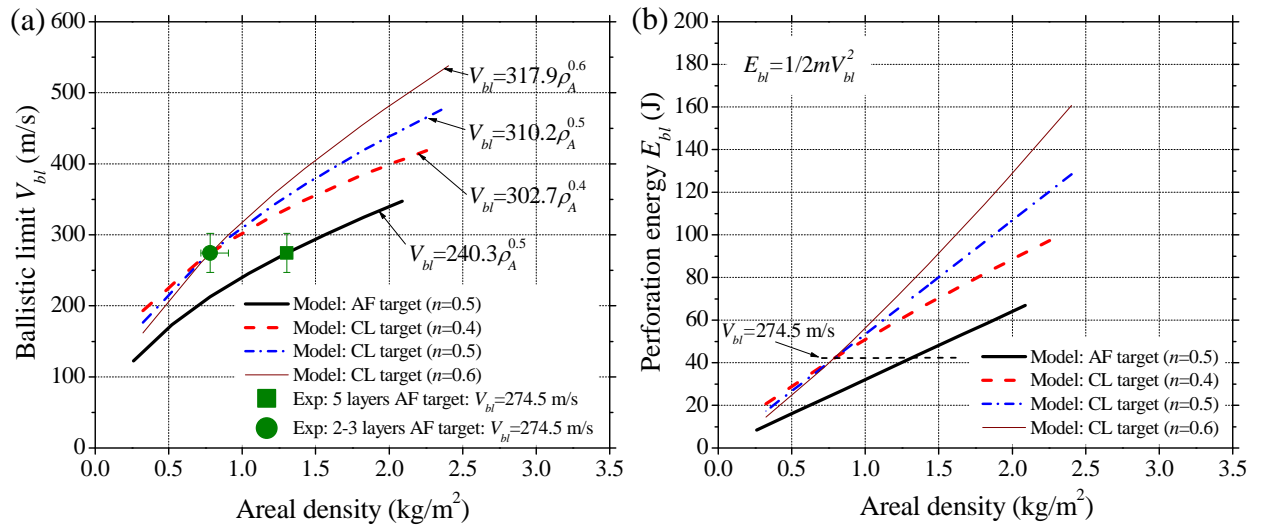


Fig. 8. (a) Predicted ballistic limit versus areal density; (b) predicted perforation threshold energy versus areal density.

#### 4. Conclusions

In this work, the ballistic performance of aramid fabric/polypropylene (PP) composite laminates (CL) and plain layered aramid fabric (AF) impact specimens was investigated. It was found that adding a thermoplastic PP matrix increases the ballistic performance of CL targets when compared to the AF targets with similar areal density. It was also found that the enhanced ballistic performance of CL targets is due to the fact that the PP matrix enables different energy-absorbing mechanisms, including a larger deformation of secondary yarns, fabric/matrix debonding, matrix cracking and delamination, which are not observed in AF systems. For AF systems, straining of primary yarns is the main mechanism of energy absorption. The ballistic limit and penetration threshold energy were predicted for both CL and AF targets using an empirical model. It was found that both the ballistic limit and perforation threshold energy increases for CL targets when compared to AF targets with a similar areal density. The findings in this study are important from a design viewpoint of soft armors because less aramid fabric is required to obtain the same level of protection when the thermoplastic PP matrix is incorporated, which may potentially lead to weight savings and lower costs. However, further studies should be carried out to confirm the results of this investigation, including more experimental work and analytical and/or numerical modeling.

#### Acknowledgements

The authors want to gratefully thank the Consejo Nacional de Ciencia y Tecnologia, CONACyT, for its funding with the project CB-2008-01-101680 to support this work.

#### References

- [1] A. Tabiei, G. Nilakantan. Ballistic Impact of Dry Woven Fabric Composites: A Review. *Appl Mech Rev* 2008; 61(1):010801.
- [2] A. Batnagar, B. Arvidson: in: *Lightweight ballistic composites, military and law-enforcement applications*. CRC Press. 2006. p. 272-304.
- [3] B.A. Cheeseman, T.A. Bogetti. Ballistic impact into fabric and compliant composite laminates. *Compos Struct* 2003; 61(1–2):161.
- [4] R. Zaera: in: *Impact Engineering of Composite Structures*. Springer Vienna. 2011. p. 305-403.
- [5] H.H. Yang. *Kevlar aramid fiber*. John Wiley & Sons. 1993.
- [6] C.H. Choi, Y.S. Ok, B.K. Kim, C.S. Ha, W.J. Cho, Y.J. Shin. Melt rheology and property of short aramid fiber reinforced polyethylene composites. *J Korean Ind Eng Chem* 1992; 3(1):81.
- [7] N.K. Naik, P. Shirao. Composite structures under ballistic impact. *Compos Struct* 2004; 66(1–4):579.
- [8] S. Bazhenov. Dissipation of energy by bulletproof aramid fabric. *J Mater Sci* 1997; 32(15):4167.
- [9] M.G. Dobb, R.M. Robson, A.H. Roberts. The ultraviolet sensitivity of Kevlar 149 and Technora fibres. *J Mater Sci*. 1993; 28(3):785.
- [10] X. Liu, W. Yu, N. Pan. Evaluation of high performance fabric under light irradiation. *J Appl Polym Sci* 2011; 120(1):552.

- [11] R. Park, J. Jang. Effect of laminate thickness on impact behavior of aramid fiber/vinylester composites. *Polym Test* 2003; 22(8):939.
- [12] R.H. Zee, C.Y. Hsieh. Energy loss partitioning during ballistic impact of polymer composites. *Polym Compos* 1993; 14(3):265.
- [13] E.M. Petrie. *Handbook of Adhesives and Sealants*. McGraw-Hill. 2000.
- [14] J.B. Mayo Jr, E.D. Wetzel, M.V. Hosur, S. Jeelani. Stab and puncture characterization of thermoplastic-impregnated aramid fabrics. *Int J Impact Eng* 2009; 36(9):1095.
- [15] Hexcel, Technical fabrics handbook. <[http://www.hexcel.com/Resources/DataSheets/Brochure-Data-Sheets/HexForce\\_Technical\\_Fabrics\\_Handbook.pdf](http://www.hexcel.com/Resources/DataSheets/Brochure-Data-Sheets/HexForce_Technical_Fabrics_Handbook.pdf)>. Accessed: 16-Jan-12.
- [16] T.J. Mulkern, M.N. Raftenberg, Kevlar KM2 yarn and fabric strength under quasi-static tension. Report ARL-TR-2865. Weapons and Materials Research Directorate, Army Research Laboratory. 2002.
- [17] M.J. King, P. Jearanaisilawong, S. Socrate. A continuum constitutive model for the mechanical behavior of woven fabrics. *Int J Solids Struct* 2005; 42(13):3867.
- [18] N.K. Naik, P. Shrirao, B.C.K. Reddy. Ballistic impact behaviour of woven fabric composites: Formulation. *Int J Impact Eng* 2006; 32(9):1521.
- [19] E.M. Parsons, T. Weerasooriya, S. Sarva, S. Socrate. Impact of woven fabric: Experiments and mesostructure-based continuum-level simulations. *J Mech Phys Solids* 2010; 58(11):1995.
- [20] H.H. Billon, D.J. Robinson. Models for the ballistic impact of fabric armour. *Int J Impact Eng* 2001; 25(4):411.
- [21] A.F. Wilde, D.K. Roylance, J.M. Rogers. Photographic Investigation of High-Speed Missile Impact upon Nylon Fabric. *Text Res J* 1973; 43(12):
- [22] B.L. Lee, J.W. Song, J.E. Ward. Failure of Spectra® Polyethylene Fiber-Reinforced Composites under Ballistic Impact Loading. *J Compos Mater* 1994; 28(13):1202.
- [23] B.L. Lee, T.F. Walsh, S.T. Won, H.M. Patts, J.W. Song, A.H. Mayer. Penetration Failure Mechanisms of Armor-Grade Fiber Composites under Impact. *J Compos Mater* 2001; 35(18):1605.
- [24] J.W. Song, G.T. Egglestone in: *Proc 19th SAMPE Int Tech Conf*, Azusa, CA, 1987. pp. 108–119.